Physics Letters B 768 (2017) 1–6

Contents lists available at ScienceDirect

Physics Letters B

www.elsevier.com/locate/physletb

Neutron spectroscopy of ^{26}Mg states: Constraining the stellar neutron source ^{22}Ne$(\alpha, n)^{25}$Mg

C. Massimi [a,b,*], S. Altstadt [c], J. Andrzejewski [d], L. Audouin [e], M. Barbagallo [f], V. Bécares [g], F. Bečvář [h], F. Belloni [i], E. Berthoumieux [i], J. Billowes [j], S. Bisterzo [k,l], D. Bosnar [m], M. Brugger [n], M. Calviani [n], F. Calviño [o], D. Cano-Ott [g], C. Carrapiço [p], D.M. Castelluccio [a], F. Cerutti [n], E. Chiaveri [i], L. Cosentino [r], M. Chin [n], G. Clai [a,q], N. Colonna [f], G. Cortés [o], M.A. Cortés-Giraldo [s], S. Cristallo [t], M. Diakaki [u], C. Domingo-Pardo [v], I. Duran [w], R. Dressler [x], C. Eleftheriadis [y], A. Ferrari [n], P. Finocchiaro [r], K. Fraval [i], S. Ganesan [z], A.R. García [g], G. Giubrone [v], I.F. Gonçalves [p], E. González-Romero [g], E. Griesmayer [aa], C. Guerrero [n], F. Gunsing [i], A. Hernández-Prieto [n,o], D.G. Jenkins [ab], E. Jericha [aa], Y. Kadi [n], F. Käppeler [ac], D. Karadimos [u], N. Kivel [x], P. Koehler [ad], M. Kokkoris [u], S. Kopecky [ae], M. Krtička [h], J. Kroll [h], C. Lampoudis [i], C. Langer [c], E. Leal-Cidoncha [w], C. Lederer [af], H. Leeb [aa], L.S. Leong [e], S. Lo Meo [a,q], R. Losito [n], A. Mallick [z], A. Manousos [y], J. Marganiec [d], T. Martínez [g], P.F. Mastinu [ag], M. Mastromarco [f], E. Mendoza [g], A. Mengoni [q], P.M. Milazzo [ah], F. Mingrone [a,b], M. Mirea [ai], W. Mondelaers [ae], A. Musumarra [r], C. Paradela [w], A. Pavlik [af], J. Perkowski [d], M. Pignatari [aj], L. Piersanti [t], A. Plompen [ae], J. Praena [s], J.M. Quesada [s], T. Rauscher [ak,al], R. Reifarth [c], A. Riego [o], M.S. Robles [w], C. Rubbia [n], M. Sabaté-Gilarte [s], R. Sarmento [p], A. Saxena [z], P. Schillebeeckx [ae], S. Schmidt [c], D. Schumann [x], G. Tagliente [f], J.L. Tain [v], D. Tarrío [w], L. Tassan-Got [e], A. Tsinganis [n], S. Valenta [h], G. Vannini [a,b], I. Van Rijs [ak], V. Variale [f], P. Vaz [p], A. Ventura [a], M.J. Vermeulen [ab], V. Vlachoudis [n], R. Vlastou [u], A. Wallner [am], T. Ware [j], M. Weigand [c], C. Weiß [aa], R. Wynants [ae], T. Wright [j], P. Žugec [m]

[a] *Istituto Nazionale di Fisica Nucleare, Bologna, Italy*
[b] *Dipartimento di Fisica e Astronomia, Università di Bologna, Italy*
[c] *Johann-Wolfgang-Goethe Universität, Frankfurt, Germany*
[d] *Uniwersytet Łódzki, Lodz, Poland*
[e] *Institut de Physique Nucléaire, CNRS-IN2P3, Univ. Paris-Sud et Paris-Saclay, 91406 Orsay Cedex, France*
[f] *Istituto Nazionale di Fisica Nucleare, Bari, Italy*
[g] *Centro de Investigaciones Energeticas Medioambientales y Tecnológicas (CIEMAT), Madrid, Spain*
[h] *Charles University, Prague, Czechia*
[i] *Commissariat à l'Énergie Atomique (CEA) Saclay - Irfu, Gif-sur-Yvette, France*
[j] *University of Manchester, Oxford Road, Manchester, UK*
[k] *INAF - Osservatorio astrofisico di Torino, Torino, Italy*
[l] *JINA (Joint Institute of Nuclear Astrophysics), University of Notre Dame, IN 46556, USA*
[m] *Department of Physics, Faculty of Science, University of Zagreb, Croatia*
[n] *European Organization for Nuclear Research (CERN), Geneva, Switzerland*
[o] *Universitat Politecnica de Catalunya, Barcelona, Spain*
[p] *Instituto Tecnológico e Nuclear, Instituto Superior Técnico, Universidade Técnica de Lisboa, Lisboa, Portugal*
[q] *Agenzia nazionale per le nuove tecnologie, l'energia e lo sviluppo economico sostenibile (ENEA), Bologna, Italy*
[r] *Istituto Nazionale di Fisica Nucleare, Laboratori Nazionali del Sud, Italy*
[s] *Universidad de Sevilla, Spain*
[t] *INAF - Osservatorio Astronomico di Collurania, Teramo, Italy*
[u] *National Technical University of Athens (NTUA), Greece*

* Corresponding author.
E-mail address: cristian.massimi@bo.infn.it (C. Massimi).

http://dx.doi.org/10.1016/j.physletb.2017.02.025

[v] Instituto de Física Corpuscular, CSIC-Universidad de Valencia, Spain
[w] Universidade de Santiago de Compostela, Spain
[x] Paul Scherrer Institut, Villigen PSI, Switzerland
[y] Aristotle University of Thessaloniki, Thessaloniki, Greece
[z] Bhabha Atomic Research Centre (BARC), Mumbai, India
[aa] Atominstitut, Technische Universität Wien, Austria
[ab] University of York, Heslington, York, UK
[ac] Karlsruhe Institute of Technology, Campus Nord, Institut für Kernphysik, Karlsruhe, Germany
[ad] Department of Physics, University of Oslo, N-0316 Oslo, Norway
[ae] European Commission JRC, Institute for Reference Materials and Measurements, Retieseweg 111, B-2440 Geel, Belgium
[af] University of Vienna, Faculty of Physics, Austria
[ag] Istituto Nazionale di Fisica Nucleare, Laboratori Nazionali di Legnaro, Italy
[ah] Istituto Nazionale di Fisica Nucleare, Trieste, Italy
[ai] Horia Hulubei National Institute of Physics and Nuclear Engineering - IFIN HH, Bucharest - Magurele, Romania
[aj] E. A. Milne Centre for Astrophysics, Dept. of Physics & Mathematics, University of Hull, United Kingdom
[ak] Department of Physics - University of Basel, Basel, Switzerland
[al] Centre for Astrophysics Research, University of Hertfordshire, Hatfield AL10 9AB, United Kingdom
[am] Department of Nuclear Physics, Research School of Physics and Engineering, The Australian National University, Canberra, Australia

ARTICLE INFO

Article history:
Received 7 July 2016
Received in revised form 9 February 2017
Accepted 12 February 2017
Available online 16 February 2017
Editor: V. Metag

Keywords:
s Process
α+^{22}Ne
Neutron spectroscopy

ABSTRACT

This work reports on accurate, high-resolution measurements of the ^{25}Mg$(n,\gamma)^{26}$Mg and ^{25}Mg(n,tot) cross sections in the neutron energy range from thermal to about 300 keV, leading to a significantly improved ^{25}Mg$(n,\gamma)^{26}$Mg parametrization. The relevant resonances for n+^{25}Mg were characterized from a combined R-matrix analysis of the experimental data. This resulted in an unambiguous spin/parity assignment of the corresponding excited states in ^{26}Mg. With this information experimental upper limits of the reaction rates for ^{22}Ne$(\alpha,n)^{25}$Mg and ^{22}Ne$(\alpha,\gamma)^{26}$Mg were established, potentially leading to a significantly higher $(\alpha,n)/(\alpha,\gamma)$ ratio than previously evaluated. The impact of these results has been studied for stellar models in the mass range 2 to 25 $M_{\odot}$.

1. Introduction

The stellar nucleosynthesis of elements heavier than iron occurs via neutron capture reactions and subsequent β decays. The so-called slow neutron capture process or *s* process [1] takes place in low and intermediate mass stars during their Asymptotic Giant Branch (AGB) phase. An additional *s*-process contribution comes in the helium-burning core and subsequent carbon-burning shell phases of massive stars. The ^{22}Ne$(\alpha,n)^{25}$Mg reaction constitutes a major neutron source for the *s* process. In AGB stars, this source is activated during a series of convective He-shell burning episodes, so-called thermal pulses, with temperatures as high as 400 MK (more than 30 keV thermal energy). Although it contributes only about 5% to the total neutron budget, this scenario determines the final abundance pattern. Hence, it is decisive for deriving information on neutron density, temperature, and pressure in the He-burning layers of AGB stars [1]. In massive stars, where thermal energies of 25 and 90 keV are reached during the He-core and C-shell burning phases, the neutron budget is by far dominated by the ^{22}Ne$(\alpha,n)^{25}$Mg reaction.

The ^{22}Ne$(\alpha,n)^{25}$Mg cross section in the temperature regime of the *s* process is affected by unknown resonance contributions. Also the competing ^{22}Ne$(\alpha,\gamma)^{26}$Mg reaction, whose cross section is also insufficiently known, adds to the persistent uncertainty of the neutron budget and the associated neutron densities during stellar nucleosynthesis. The (α,γ) reaction contributes to the destruction of ^{22}Ne during the entire helium burning phase because of its positive Q-value of 10.615 MeV, already before the threshold for neutron production via ^{22}Ne$(\alpha,n)^{25}$Mg ($Q=-478$ keV) is reached. In this context, the ^{25}Mg$(n,\gamma)^{26}$Mg reaction plays a non-negligible role as well, because the high *s* abundance of ^{25}Mg makes it a significant neutron poison for the *s* process. So far, this reaction rate is too uncertain for a quantitative assessment of the poisoning effect [2].

Experimental data for the ^{22}Ne$(\alpha,n)^{25}$Mg cross section are essentially limited to α energies above about 800 keV. At lower energies the most recent direct measurements [3–5] provided only an upper limit of about 10^{-11} barn, corresponding to the experimental sensitivity. The lowest resonance observed in direct measurements is at $E_{\alpha}^{Lab}=832\pm2$ keV (*e.g.* Ref. [4]).

2. Indirect approach

Since a direct approach is exceedingly difficult, indirect and transfer reactions were considered as an alternative way for constraining the reaction rate at low energies. For instance, the α-transfer reaction ^{22}Ne(^{6}Li, d)^{26}Mg has been studied [5–7] to search for levels in ^{26}Mg also below the neutron threshold at 11.093 MeV. These studies are particularly relevant for estimating the ^{22}Ne$(\alpha,\gamma)^{26}$Mg rate, where levels below and above the neutron threshold are involved. Direct ^{22}Ne$(\alpha,\gamma)^{26}$Mg measurements have only been carried out above 0.8 MeV. In view of the scarce experimental information, evaluations had, therefore, to rely on theoretical estimates. Accordingly, the uncertainties of the stellar ^{22}Ne$(\alpha,n)^{25}$Mg and ^{22}Ne(α,γ) rates are still dominated by unknown properties of states in the compound nucleus ^{26}Mg above the α threshold at 10.615 MeV.

As indicated in Fig. 1, these states can be studied via neutron resonance spectroscopy of n+^{25}Mg. In particular, a simultaneous resonance shape analysis of total and capture cross section data can be used to determine the resonance energies, E_R, spin parities, J^{π}, as well as the capture and neutron widths Γ_{γ} and Γ_n [8]. Information from previous ^{25}Mg$(n,\gamma)^{26}$Mg measurements suffers from considerable uncertainties due to sample problems and counting statistics. Moreover, the available transmission data have been obtained with natural Mg samples, a serious limitation in view of the dominant abundance of ^{24}Mg in natural magne-

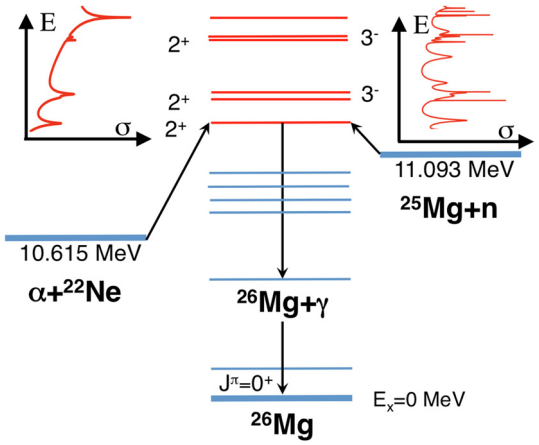

Fig. 1. Level scheme (not to scale) of ^{26}Mg with the entrance channels ^{22}Ne+α and n+^{25}Mg and the exit channel ^{26}Mg+γ. Excited states in ^{26}Mg with natural parity (0^+, 1^-, 2^+, ...) and energies below $E_\alpha^{Lab} = 850$ keV (in red) can be studied via neutron resonance spectroscopy of n+^{25}Mg as indicated by the schematic ^{25}Mg$(n,\gamma)^{26}$Mg cross section. (Color online.)

sium. The corresponding differences between present and previous transmission results are discussed in Ref. [9].

3. Measurements of n+^{25}Mg

This work on n+^{25}Mg combined two neutron time-of-flight measurements, using the CERN-n_TOF facility [10] for the (n,γ) channel and the GELINA accelerator at IRMM/Geel [11] for the total cross section. To avoid the limitations of previous attempts, both measurements were carried out with highly enriched, metallic samples (97.87% ^{25}Mg). The n_TOF facility, which provides a white neutron spectrum from thermal energy to about 1-GeV neutron energy, was chosen because it is particularly well suited for accurate high-resolution neutron measurements due to its outstanding instantaneous neutron flux (about 10^6 neutrons per bunch at the experimental area) and the very long flight-path of 185 m. The experimental setup was based on two deuterated benzene (C_6D_6) scintillation detectors (cylindrical cells with an active volume of about 1 liter), placed on either side of the neutron beam, 9.0 cm upstream of the sample. These detectors are characterized by a very small neutron sensitivity. The chosen geometrical configuration minimized the background due to scattered in-beam γ rays and reduced systematic effects due to the anisotropy in the angular distribution from primary γ-rays following p-wave neutron resonances. The total number of neutrons impinging on the various samples used in the measurement was determined by means of a low-mass, ^{6}Li-based, neutron detector [12], while the energy dependence of the neutron flux derived from a dedicated study [13]. The well-established total energy detection principle in combination with the pulse height weighting technique [14] was applied to make the detection efficiency for a capture event directly proportional to the total γ-ray energy available in the capture event. Moreover the saturated resonance technique [14] was used to normalize the capture data. The measurement covered the energy range from thermal energy to about 300 keV with a resolution of 0.05% to 0.3% in the relevant energy range between 1 and 300 keV.

The total cross section of n+^{25}Mg was measured with a ^{6}Li-glass detector at the 50 m station of the GELINA facility for energies up to about 300 keV. A combination of Li-carbonate plus resin, Pb and Cu-collimators was used to reduce the neutron beam to a diameter of less than 35 mm at the sample position. The sample was placed in an automatic sample changer at a distance of 23.78 m from the neutron source. Close to the sample position a ^{10}B anti-overlap filter was placed to absorb slow neutrons from a previous burst. In order to have a well-characterized measurement condition, permanent Na and Co black resonance filters [14] were used to continuously monitor the background at 2.85 keV and 132 eV. Additional black resonance filters were used in dedicated runs. Thanks to the small dimensions of the neutron-producing target and the excellent time characteristic (1-ns pulse width), GELINA is particularly suited for high-resolution transmission measurements in the keV region.

Essential improvements with respect to the previous capture measurement at n_TOF [2] are the quality of the highly enriched ^{25}Mg sample and a substantially reduced background of in-beam γ rays [10]. The total cross section measurement benefits also significantly from the highly enriched sample. In both measurements the experimental background was determined in dedicated runs.

The data reduction for the determination of the cross section starting from detectors counting rate was performed following the procedures described in [14]. The capture yield (representing the fraction of the neutron beam undergoing capture events) obtained at n_TOF and the transmission (representing the fraction of neutron beam that traverses the sample without interaction) from GELINA are presented in Fig. 2 and compared with the results of a simultaneous R-matrix analysis of both data sets. More in detail, the experimental capture yield Y, deduced from the response of the capture detection system and the flux-monitor is related to the total and capture cross-sections, σ_{tot} and σ_γ respectively, by the following expression [14]:

$$Y(E_n) = (1 - e^{-n_C \sigma_{tot}(E_n)}) \frac{\sigma_\gamma(E_n)}{\sigma_{tot}(E_n)} + Y_{MS}(E_n), \quad (1)$$

while the transmission T, which was experimentally obtained from the ratio of Li-glass spectra resulting from a sample-in and a sample-out measurement, is related to the total cross-section by [14]:

$$T(E_n) = e^{-n_T \sigma_{tot}(E_n)}, \quad (2)$$

where $n_C = (3.012 \pm 0.009) \times 10^{-2}$ atoms/b denotes the areal density of the capture sample and $n_T = (5.02 \pm 0.04) \times 10^{-2}$ atoms/b the one of the transmission sample, E_n the laboratory neutron energy, and Y_{MS} the contribution of multiple interaction in the sample. This latter term, together with other experimental effects such as self-shielding, Doppler broadening and response of the time-of-flight spectrometer, are properly taken into account in the R-Matrix codes SAMMY [15] and REFIT [16] used in the present combined analysis.

4. Improved ^{25}Mg$(n,\gamma)^{26}$Mg cross section

Resonance energies, E_R, partial widths, Γ_γ and Γ_n, and the spins and parities, J^π were determined by a combined R-matrix analysis in the energy region $E_n < 300$ keV, corresponding to an incident α-particle energy from threshold at $E_\alpha = 570$ keV to approximately 850 keV, where direct (α, n) measurements are difficult and accurate cross section data are missing.

The information on J^π is particularly important for identifying the states in ^{26}Mg that contribute to the ^{22}Ne$(\alpha,n)^{25}$Mg cross section. This selection is crucial because ^{22}Ne nuclei and α particles have both $J^\pi = 0^+$. Accordingly, (α, n) reactions can only populate natural-parity states ($0^+, 1^-, 2^+, \ldots$) in ^{26}Mg, whereas the n+^{25}Mg reaction proceeds also via $J^\pi = 1^+, 2^-, 3^+, \ldots$ states.

The results of the combined R-matrix analysis of both cross sections are summarized in Table 1, including the deduced firm J^π assignments. For the natural-parity states, the α energies in the laboratory system E_α^{Lab} are given in column 3 for comparison

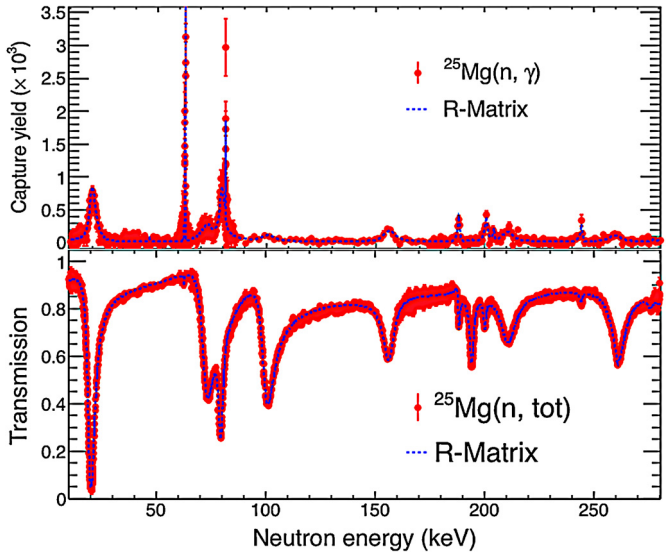

Fig. 2. Measured neutron capture yield and transmission of ^{25}Mg. Experimental data are represented by red symbols and the simultaneous R-matrix of both data sets is given by dashed lines. (Color online.)

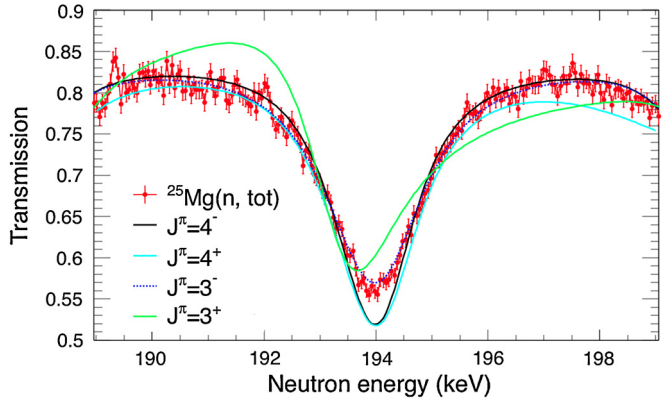

Fig. 3. Resonance shape analysis of the neutron resonance at $E_n = 194$ keV. The spin parity assignment $J^\pi = 4^-$ [17] is excluded by the present data, which clearly indicate $J^\pi = 3^-$. Only uncorrelated uncertainties, attributable to counting statistics, are reported. (Color online.)

with direct α+^{22}Ne measurements. The uncertainties on E_x and E_α^{Lab} are determined by the uncertainty in neutron energy, which never exceeds 0.1 keV. This is an important result in itself because it allows one to resolve inconsistencies in charged-particle data.

Fig. 3 demonstrates the sensitivity of the present data to spin and parity, which clearly exclude the previous $J^\pi = 4^-$ assignment [17] for the neutron resonance at 194 keV. In particular, the lowest values of the chi-squared per number of degrees of freedom of the fit, were 1.1, 5.6, 7.3 and 17 assuming $J^\pi = 3^-$, 4^+, 4^- and 3^+ respectively. In this manner the J^π values were determined for each resonance. In two cases the spin-parity assignment was changed with respect to the previous evaluation. As shown in Ref. [9], these two resonances could not be accurately studied by using the transmission data on natural magnesium (*e.g.* reported in [17]) since the experimental signature was dominated by strong resonances in n+^{24}Mg.

Compared to evaluated resonance data [18], six neutron resonances had to be removed in the energy range covered in Table 1. These weak resonances ($\Gamma_n \approx 0.5$ eV) were assigned in previous n+^{25}Mg experiments, but were not identified in this work.

Table 1
n+^{25}Mg resonance parameters and corresponding excitation energies of the ^{26}Mg compound nucleus. The quoted uncertainties were obtained by the R-Matrix fit.

E_n (keV)	E_x (keV)	E_α^{Lab} (keV)	J^π ($\hbar$)	Γ_γ (eV)	Γ_n (eV)
19.92(1)	11112	589	2^+	1.37(6)	2095(5)
62.73(1)	11154		1^+	4.4(5)	7(2)
72.82(1)	11163	649	2^+	2.8(2)	5310(50)
79.23(1)	11169	656	3^- [a]	3.3(2)	1940(20)
81.11(1)	11171			5(1)	1–30
100.33(2)	11190		3^+	1.3(2)	5230(30)
155.83(2)	11243		2^-	4.7(5)	5950(50)
187.95(2)	11274	779	2^+	2.2(2)	410(10)
194.01(2)	11280	786	3^- [a]	0.3(1)	1810(20)
199.84(2)	11285		2^-	4.8(4)	1030(30)
203.88(4)	11289			0.9(3)	3–20
210.23(3)	11295		2^-	6.6(6)	7370(60)
243.98(2)	11328	(843)		2.2(3)	171(6)
260.84(8)	11344			1.0(2)	300–3900
261.20(2)	11344		> 3	3.0(3)	6000–9000

[a] Parity change with respect to previous evaluations.

Below the lowest directly observed resonance in the ^{22}Ne$(\alpha, n)^{25}$Mg reaction cross-section at $E_\alpha^{Lab} \approx 830$ keV ($E_n \approx 235$ keV), five natural-parity states have been identified corresponding to energies $E_\alpha^{Lab} = 589$, 649, 656, 779 and 786 keV. The doublets at 649/656 and 779/786 keV were resolved owing to the good energy resolution in the neutron channel, which is significantly better than in charged-particle experiments. The lowest observed ^{22}Ne$(\alpha, n)^{25}$Mg resonance at $E_\alpha^{Lab} = 832 \pm 2$ keV [4] was not observed in the present neutron data at $E_n = 234$ keV, while a resonance with a width compatible to the one reported in [4] ($\Gamma = 250 \pm 170$ eV) is located at $E_n = 243.98$ keV, *i.e.* $E_\alpha^{Lab} = 843$ keV. One possible explanation is that the two resonances correspond to the same state, in which case the energies are inconsistent with each other. Another possibility is that they correspond to two different levels: in this case the width of the (α, n) resonance at 832 keV is lower than quoted in [4], being below the sensitivity of the present measurements ($\Gamma \approx 20$ eV), while the observed neutron level is not a natural parity state.

The ^{25}Mg$(n, \gamma)^{26}$Mg cross section was also significantly improved by an R-matrix analysis of the combined data sets for ^{25}Mg(n, γ) and (n, tot), resulting in rather accurate Maxwellian averaged cross section (MACS) for thermal energies between $kT =$ 5 and 100 keV. Though higher resonances up to 900 keV were considered as well, the MACS values are dominated by contributions from the resonances in Table 1. The present results and the currently recommended values in the KADoNiS [22] compilation and in Ref. [2] are compared in Table 2. While the new MACS values are compatible with the previous measurement [2] except for the lowest and highest temperature, the uncertainties were reduced by almost a factor of three on average. These uncertainties are the sum of uncorrelated or statistical uncertainties and systematic uncertainties.

5. Impact on reaction rate calculations

As mentioned above, the reaction channels for α+^{22}Ne and n+^{25}Mg open at excitation energies $E_x = 10.615$ and 11.093 MeV in the compound nucleus ^{26}Mg. Apart from the levels between α- and n-channel, the present study provides access to the relevant states in the energy region between the ^{22}Ne$(\alpha, n)^{25}$Mg threshold and the lowest resonance reached in direct α+^{22}Ne experiments. Therefore the new resonance information has been used for calculating the upper limit of the reaction rates, based purely on experimentally-available information for ^{22}Ne$(\alpha, n)^{25}$Mg and

Table 2
^{25}Mg(n, γ) Maxwellian-averaged cross sections (in mb), compared with a previous work and recommended values. Experimental values include the contributions from direct radiative capture [2].

kT (keV)	5	10	15	20	25	30	40	50	60	80	100
KADoNiS	4.8	5.0	5.5	6.0	6.2	6.4(4)	6.2	5.7	5.3	4.4	3.6
Ref. [2]	3.5(4)	5.1(6)	4.9(6)	4.6(4)	4.4(6)	4.1(6)	3.5(6)	2.9(5)	2.5(4)	1.9(3)	1.4(2)
this work	2.8(2)	4.4(2)	4.3(2)	4.2(2)	4.0(2)	3.9(2)	3.6(2)	3.4(2)	3.0(2)	2.5(3)	2.2(3)

^{22}Ne$(\alpha,\gamma)^{26}$Mg. In particular, they were defined using: (i) data from an α-transfer reaction for the resonance below the neutron threshold [7], (ii) data from this work, and (iii) data from direct measurements above $E_\alpha^{Lab} = 800$ keV [4]. The calculation, based on the simple narrow-resonance formalism [23], requires as input the resonance energies and the so-called kernels (also referred to as resonance strength), k_n or k_γ,

$$k_n = g\frac{\Gamma_\alpha\Gamma_n}{\Gamma},$$
$$k_\gamma = g\frac{\Gamma_\alpha\Gamma_\gamma}{\Gamma} = k_n\frac{\Gamma_\gamma}{\Gamma_n}; \quad (3)$$

where Γ is the total width and $g = (2J+1)/[(2I+1)(2i+1)]$ the statistical factor and J, I and i the spin of the resonance, target and projectile, respectively. Because $\Gamma_\alpha \ll \Gamma_\gamma \ll \Gamma_n$, the kernels can be reduced to $k_n = g\Gamma_\alpha$.

Apart from Γ_α, all quantities were determined in this work. For the present analysis we estimated the upper limits of Γ_α based on the experimental constraint on the ^{22}Ne$(\alpha,n)^{25}$Mg cross section ($\leq 10^{-11}$ barn, corresponding to $\Gamma_\alpha \approx 10^{-8}$ eV).

The contributions of the five resonances below $E_\alpha^{Lab} \approx 800$ keV to the ^{22}Ne$(\alpha,n)^{25}$Mg rate depend on the temperature of the specific s-process site. Particularly important is the 30% decrease of the upper limit of the rate compared to Ref. [7] around $kT =$ 25 keV (0.25 to 0.3 GK in Fig. 4), which affects the neutron economy during the He shell burning in low-mass AGB stars and during core He burning in massive stars.

The neutron resonance data obtained in this work were also used to determine the upper limit of the ^{22}Ne$(\alpha,\gamma)^{26}$Mg rate. As shown in Fig. 4, these results differ significantly compared to recent evaluations [7,19,20], also in the important temperature range above 0.3 GK. Part of these discrepancies were caused by a misinterpretation of previous neutron data, in particular for the doublet at $E_n = 79$ keV. While the impact of the 79-keV doublet on the ^{22}Ne$(\alpha,n)^{25}$Mg rate is relatively small (at most 3%), it plays a major role for the (α,γ) rate. As discussed in Ref. [7], α-transfer measurements provide experimental evidence of a natural parity state in ^{26}Mg corresponding to an energy of about $E_n = 80$ keV. Prior to this measurement the resonance at $E_n = 79$ keV was tentatively assigned to be of unnatural parity whereas the closest resonance at $E_n = 81$ keV was considered as the one with natural parity. This misinterpretation resulted in a biased ^{22}Ne$(\alpha,\gamma)^{26}$Mg reaction rate, since the resonance strength of the (α,γ) channel scales with the Γ_n/Γ_γ ratio (see Eq. (3)). With the present spin-parity assignment, the contribution to the reaction rate of this level became negligible since the Γ_n/Γ_γ ratio of the resonance at $E_n = 79$ keV is about a factor of 2200 larger than the ratio of the resonance at $E_n = 81$ keV.

In summary, the present resonance analysis of the neutron-induced cross sections of ^{25}Mg has led to decisive improvements for the poorly known states in ^{26}Mg with excitation energies between 11112 and 11344 keV. This concerns accurate level energies, firm spin/parity assignments, and the determination of reliable Γ_γ and Γ_n values. The conclusive identification of their properties were used to determine the contributions of levels below the energy range covered by direct (α,n) measurements. While waiting for the crucial estimate of Γ_α, which will require a large experimental effort, the present results can lead to improvements in the calculation of the stellar ^{22}Ne+α rates in the astrophysically relevant energy range substantially. In particular, it was found that the (α,γ) channel had been strongly overestimated so far. The present results are summarized in Table 3.

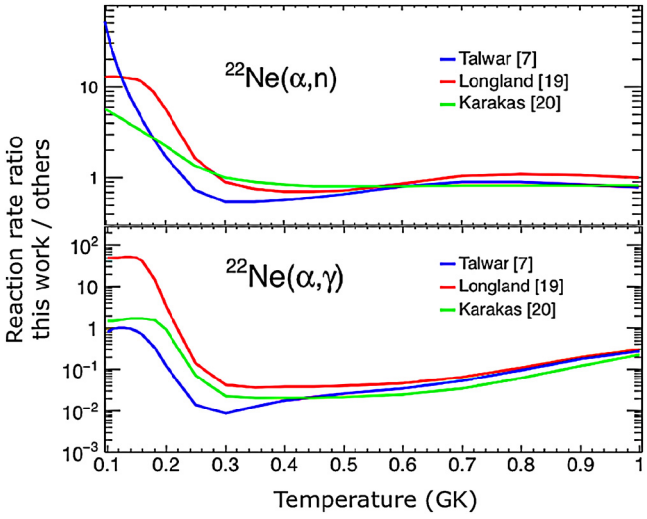

Fig. 4. Reaction rate ratio of the upper limits for the ^{22}Ne$(\alpha,n)^{25}$Mg (top panel) from this work compared to the upper limits in Refs. [7,20,19]. The same ratios are presented for the ^{22}Ne$(\alpha,\gamma)^{26}$Mg (bottom panel). Below 0.3 GK the present data are indicating an enhanced (α,n) rate, whereas the (α,γ) rate is strongly reduced above that temperature. (Color online.)

Table 3
Upper limits of the reaction rates, given in cm^3/(mole s), determined from the present measurements.

Temperature	Upper limits	
10^9 K	^{22}Ne(α,n)	^{22}Ne(α,γ)
0.06	2.97×10^{-44}	4.13×10^{-21}
0.08	5.56×10^{-34}	8.45×10^{-28}
0.10	7.56×10^{-28}	3.23×10^{-24}
0.12	8.96×10^{-24}	1.55×10^{-21}
0.13	3.29×10^{-22}	1.67×10^{-20}
0.14	7.16×10^{-21}	1.27×10^{-19}
0.15	1.04×10^{-19}	7.35×10^{-19}
0.16	1.07×10^{-18}	3.39×10^{-18}
0.18	5.32×10^{-17}	4.27×10^{-17}
0.19	2.78×10^{-16}	1.23×10^{-16}
0.20	1.25×10^{-15}	3.21×10^{-16}
0.25	4.99×10^{-13}	1.43×10^{-14}
0.30	4.52×10^{-11}	5.82×10^{-13}
0.35	1.44×10^{-09}	1.82×10^{-11}
0.40	2.09×10^{-08}	2.66×10^{-10}
0.45	1.74×10^{-07}	2.12×10^{-09}
0.50	1.03×10^{-06}	1.15×10^{-08}
0.60	2.24×10^{-05}	1.50×10^{-07}
0.70	3.36×10^{-04}	1.18×10^{-06}
0.80	3.19×10^{-03}	7.38×10^{-06}
0.90	1.95×10^{-02}	3.67×10^{-05}
1.00	8.45×10^{-02}	1.43×10^{-04}

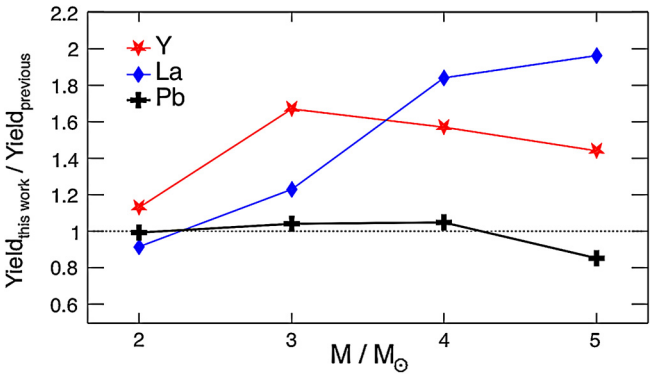

Fig. 5. Ratios of the *s* abundance of Y, La, and Pb from stellar *s*-process models using the present upper limits of the ^{22}Ne$(\alpha,n)^{25}$Mg rate and from the FRUITY reference set [24].

6. Astrophysical implications and conclusions

The astrophysical consequences of the present results have been studied using the upper limits established in this work. Their impact on the weak-s process in massive stars was explored for a 25 $M_\odot$ [21] star. The calculated abundances are consistent with the latest evaluations [7,19]. The present uncertainty of the $\alpha+^{22}$Ne rate causes large differences in the weak s-process abundances, up to a factor 50 in the Sr region.

Noticeable changes are also found in intermediate-mass AGB models (IMS-AGBs, $3 < M/M_\odot < 7$). As in these stars higher temperatures are reached during thermal pulses than in low-mass AGB stars, the strong preponderance of the ^{13}C$(\alpha,n)^{16}$O neutron source is progressively substituted by the ^{22}Ne$(\alpha,n)^{25}$Mg reaction. This is particularly evident at low metallicities.

Using the present upper limits for the ^{22}Ne(α,n) rates, the *s*-process yields of AGB stars between 2 and 5 $M_\odot$ and an initial iron fraction corresponding to 0.7% of the solar value were calculated for comparison with reference AGB models from the FRUITY data base [24]. The resulting *s* abundances of Y and La were selected for comparison with Pb, because Y and La are characterizing the first and second *s*-process abundance peak. As illustrated in Fig. 5 the production of Y and – especially – of La is increasing with AGB mass as a consequence of the more efficient ^{22}Ne$(\alpha,n)^{25}$Mg source, whereas the Pb abundance remains basically frozen. For a fixed amount of Pb we obtain, therefore, larger abundances in the first and, especially, in the second *s*-process peak. This pattern in higher-mass stars may help to explain the surface distributions in *s*-process enriched globular cluster stars, which exhibit a comparably low Pb abundance [25]. Whether a mix of enhanced *s* contributions from IMS-AGBs at the expense of the Pb producing LMS-AGBs could provide a plausible solution will be analyzed in a dedicated paper.

Acknowledgements

The isotope used in this research were supplied by the United States Department of Energy Office of Science by the Isotope Program in the Office of Nuclear Physics.

M. Pignatari and I. Van Rijs thank NuGrid for the support.

References

[1] F. Käppeler, R. Gallino, S. Bisterzo, W. Aoki, Rev. Mod. Phys. 83 (2011) 157.
[2] C. Massimi, et al., Phys. Rev. C 85 (2012) 044615.
[3] H.W. Drotleff, et al., Astrophys. J. 414 (1993) 735.
[4] M. Jaeger, R. Kunz, A. Mayer, J.W. Hammer, G. Staudt, K.L. Kratz, B. Pfeiffer, Phys. Rev. Lett. 87 (2001) 202501.
[5] U. Giesen, et al., Nucl. Phys. A 561 (1993) 95.
[6] C. Ugalde, et al., Phys. Rev. C 76 (2007) 025802.
[7] R. Talwar, et al., Phys. Rev. C 93 (2016) 055803.
[8] F.H. Fröhner, Evaluation and Analysis of Nuclear Resonance Data, JEFF Report 18, NEA/OECD, 2000.
[9] C. Massimi, et al., EPJ Web Conf. 66 (2014) 07016.
[10] C. Guerrero, et al., Eur. Phys. J. A 49 (2013) 27.
[11] W. Mondelaers, P. Schillebeeckx, Notiziario 11 (2006) 19.
[12] S. Marrone, et al., Nucl. Instrum. Methods A 517 (2004) 389.
[13] M. Barbagallo, et al., Eur. Phys. J. A 49 (2013) 156.
[14] P. Schillebeeckx, et al., Nucl. Data Sheets 113 (2012) 3054.
[15] N.M. Larson, Updated Users Guide for SAMMY: Multilevel Rmatrix Fits to Neutron Data Using Bayes Equations, SAMMY, Computer Code, Report No. ORNL/TM-9179/R7, Oak Ridge National Laboratory, 2008.
[16] M.C. Moxon, J.B. Brisland, GEEL REFIT, A least squares fitting program for resonance analysis of neutron transmission and capture data computer code, in: InTec-0630, AEA Technology, October 1991.
[17] P.E. Koehler, Phys. Rev. C 66 (2002) 055805.
[18] S.F. Mughabghab, Atlas of Neutron Resonances, Elsevier, Amsterdam, 2006.
[19] R. Longland, C. Iliadis, A.I. Karakas, Phys. Rev. C 85 (2012) 065809.
[20] A.I. Karakas, M.A. Lugaro, M. Wiescher, J. Görres, C. Ugalde, Astrophys. J. 643 (2006) 471.
[21] R. Hirschi, U. Frischknecht, M. Pignatari, et al., NuGrid: *s* process in massive stars, in: Proc. of Nuclei in the Cosmos (NIC X), Mackinac Island, Michigan, USA, 2008.
[22] I. Dillmann, R. Plag, F. Käppeler, and T. Rauscher, in: Proceeding of the workshop "EFNUDAT Fast Neutrons – Scientific Workshop on Neutron Measurements, Theory & Applications", April 28–30, 2009, Geel, Belgium.
[23] C.E. Rolfs, W.S. Rodney, Cauldrons in the Cosmos, University of Chicago Press, Chicago, 1988.
[24] S. Cristallo, O. Straniero, L. Piersanti, D. Gobrecht, Astrophys. J. Suppl. Ser. 219 (2015) 40.
[25] O. Straniero, S. Cristallo, L. Piersanti, Astrophys. J. 785 (77) (2014).